Chemical Physics 56 (1981) 157–165
North-Holland Publishing Company

MULTIPHOTON IONIZATION TRANSLATIONAL SPECTROSCOPY (MITS) OF I_2

M.S. DE VRIES, N.J.A. VAN VEEN, T. BALLER and A.E. DE VRIES
FOM-Institute for Atomic and Molecular Physics, Amsterdam/Wgm., The Netherlands

Received 6 October 1980

A new technique is introduced based on the measurement of kinetic energies and angular distributions of fragments in multiphoton ionization of molecules. Both positive and negative ions are measured as well as neutrals. Information is obtained about highly excited repulsive states and about the multiphoton ionization process itself. Examples are reported for MPI of I_2. In a one-laser experiment dissociative autoionization is observed. In a two-laser experiment processes are distinguished, that have different intermediate states. Lifetimes of those states are measured. Information is also obtained about an ion pair formation process, leading to a reinterpretation of potential curves.

1. Introduction

Multiphoton ionization of molecules became of considerable interest when suitable lasers made the subject experimentally accessible [1]. The reason for this interest is not only in the multiphoton process itself. There are also two significant practical considerations:

(i) Multiphoton ionization is used as a new spectroscopic tool. The ionization permits sensitive detection of highly excited bound states via resonant excitation.

(ii) Resonance enhanced multiphoton ionization is proposed as a state selective detection scheme.

The first experiments in the field were bulk experiments in which the total amount of ions formed was measured as a function of laser wavelength and sometimes of laser intensity and polarization [2]. The technique was extended by the use of two lasers and by the introduction of molecular beams [3]. It was further modified by the use of a mass filter in order to distinguish molecular ions from fragment ions [4]. We now introduce a new approach by measuring kinetic energies and angular distributions of ionic and neutral fragments formed. The basic consideration involved here is the following. Although in multiphoton ionization the intermediate states are discrete the final steps always involve a continuum. Excess energy can be carried away by a photo-electron and often by fragments. Observation of those fragments can yield information concerning highly excited repulsive states and also concerning the process itself. For example if different fragmentation processes occur simultaneously they can be distinguished by the fact that they produce fragments with different kinetic energies.

We have chosen I_2 to demonstrate the principle, both for experimental convenience and because it is a well documented system. Much is known about its spectroscopy [5] and there are several multiphoton experiments done on iodine along the "conventional" lines [6,7]. Bernstein and co-workers [6d] studied multiphoton dissociation of I_2 and several other compounds. They did not perform velocity distributions. One of the many results found by them is that the process of resonance enhanced multi-photon ionization "does not follow the least energetically demanding route to ion formation". To understand the reason for this is one of the goals of the type of study presented here.

Tai and Dalby [6c], dissociating molecular iodine, found fluorescence from I atoms, leading them to a knowledge of the electronic state. In this respect their method is complementary to ours. The fact that they found dissociation into $I + I^*$ (see fig. 5) means diabatic behaviour and is in accordance with the calcu-

0 301–0104/81/0000–0000/$02.50

lated behaviour as discussed in section 4.

A study of Na_2 multiphoton ionization similar in spirit to the one described here has been published by Nitz et al. [7]. They use an extraction voltage for the ions, small enough to differentiate between Na^+ and Na_2^+. Because they have only one outgoing channel this suffices for the analysis. The fragmentation process is governed by an energy balance:

$$E_{\text{frag}} = n_1 h\nu_1 + n_2 h\nu_2 - D(v, J) - E_{\text{int}} - E_{\text{el}} . \quad (1)$$

E_{frag} is the energy available for translation of the fragments. The molecule absorbs n_1 photons of frequency ν_1 and — in a two-laser experiment — also n_2 photons of frequency ν_2. $D(v, J)$ is the dissociation energy from the vth vibrational and the Jth rotational state of the ground state molecule. E_{int} is the internal energy of the fragments. E_{el} is the kinetic energy of the photoelectron (if any). Measurement of fragment kinetic energies gives insight in the processes that occur. It yields combined information about the outgoing channels (E_{int}) and about n_1 and n_2. The latter information can sometimes be derived from the dependence of the signal on laser power, but not always because transitions are often saturated. Denoting the total absorbed energy by E we schematically list the main fragmentation processes:

$$I_2 + E \rightarrow (I_2^* \rightarrow) \begin{cases} I + I \\ I + I^* ; \\ I^* + I^* \end{cases} \quad (I)$$

$$I^* + h\nu \rightarrow I^+ + e , \quad (I')$$

$$I_2 + E \rightarrow (I_2^* \rightarrow) I^+ + I^- , \quad (II)$$

$$I_2 + E \rightarrow (I_2^* \rightarrow) I_2^+ + e ; \quad (III)$$

$$I_2^+ (+ h\nu) \rightarrow I^+ + I . \quad (III')$$

Steps in parentheses are optional. In processes (I) and (II) the energy balance is maintained, while in process (III) excess energy can be carried away by a photoelectron. This can be observed in the experiment as it leads to broader energy distributions for the fragment kinetic energy E_{frag}.

2. Experimental procedure

The apparatus is an extension of an apparatus described elsewhere [8]. Fig. 1 gives a schematic diagram. Two pulsed lasers are fired from opposite directions and perpendicularly to a thermal molecular beam,

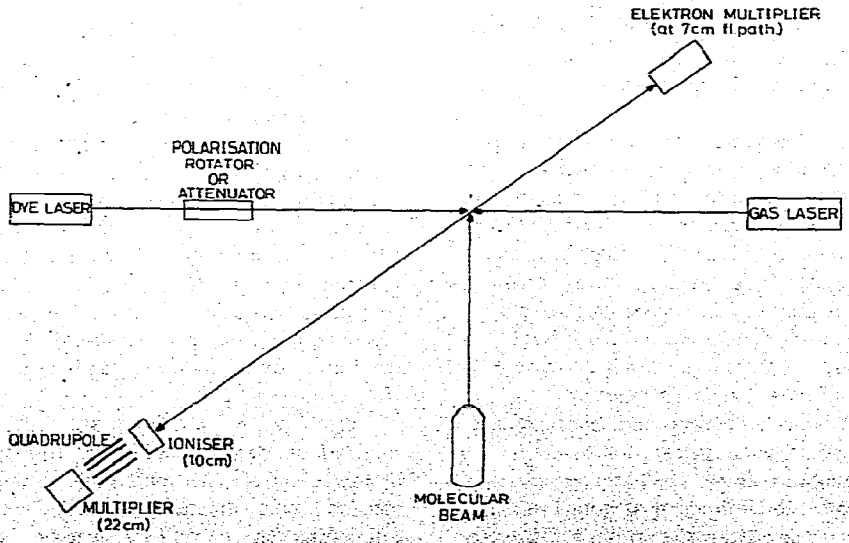

Fig. 1. Schematic diagram of the experimental arrangement.

onto which they are focused by means of two suprasil lenses to a spot of 0.1 cm^2. One laser is a dye laser producing 5 mJ pulses of 1.5 μs duration. The light is polarized and the direction of the electric field vector can be rotated. The other is an excimer laser producing 100–200 mJ pulses in 20 ns. The light was usually unpolarized but a polarizer could be inserted. The delay between the two lasers can be varied and the firing of the second laser triggers a CAMAC multichannel analyser module. Spectra of fragment intensities are recorded as a function of flight time. From this kinetic energies are obtained. The fragments are detected perpendicularly to molecular and laser beams in either one or three detector configurations:

(1) An electron multiplier at a 69 mm flight path from the interaction centre for observing ionic fragments with a large solid angle.

(2) A detection chamber containing an ionizer–quadrupole–multiplier arrangement for detecting neutral fragments at a 100 mm flight path.

(3) With grounded ionizer and quadrupole the detection chamber can also be used to observe ionic fragments with a small solid angle an at a 220 mm flight path.

Negative ions are observed by reversing the voltages at the ion detectors. We have performed two types of experiments. (I) A one laser–two photon experiment with 193 nm radiation from the ArF line of the multigas excimer laser. (II) A two-laser experiment with ≈585 nm from the dye laser plus 248 nm from the KrF line of the excimer laser. The latter experiment permitted information to be gained about intermediate states, excited by the initiating laser. The excited molecule was subsequently ionized by the probe laser. Neither one of the lasers alone could ionize the ground state molecule.

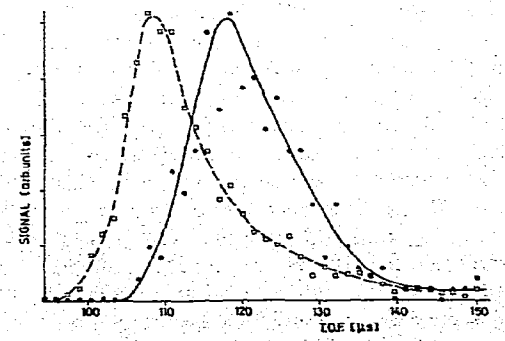

Fig. 2. Flight time spectra showing the effect of space charge in the interaction centre. Two spectra are shown (normalized to the same maximum) of arrival times of I^+ ions after the ionizing laser shots. The faster ion signal is obtained with larger molecular beam density, and therefore larger ion density in the interaction region.

Care must be taken to avoid some experimental problems, the most important one being the possibility of creating a space charge in the interaction region by producing too many ions. The result is a net acceleration of the fragments, invalidating any measurement of kinetic energy. Fig. 2 shows two time of flight spectra for the same process, obtained with different molecular beam densities. (Both peaks are normalized to the same maximum.) The faster fragments result from a higher ion density in the interaction center. From our data we estimate an upper limit for the maximum allowable ion density of 10^6 ions per cm^3. At higher densities space charge made determinations of fragment energies unreliable. This sets an upper limit to count rates and necessitates the use of a large solid angle in most experiments. However, in that configuration background ions are observed which are formed by the powerful excimer laser either at surfaces or in the residual gas. This poses a problem since this background is not spaced uniformly in time after the laser shot. For these reasons we have employed different configurations for different experiments: (a) The small solid angle was used in the one-laser experiments for studying processes that are not affected by space charge, as will be explained below. (b) The large solid angle was used with two lasers as follows: The initiating laser was turned on and off alternatively by computer control. Afterwards the sampled background measured in the "off" periods was subtracted from the signal obtained in the "on" periods. In this way background free spectra were obtained. The probability that a fragment with a certain velocity reaches the detector depends upon the distributions of molecular velocities and rotations, on the fragment kinetic energy and on the solid angle of the detector. Because of this a deconvolution is necessary. It is described in ref. [8] and more extensively in ref. [14].

3. Results and discussion — one laser

I_2 was irradiated with 193 nm photons (6.42 eV). Ionic fragments were observed by the multiplier at

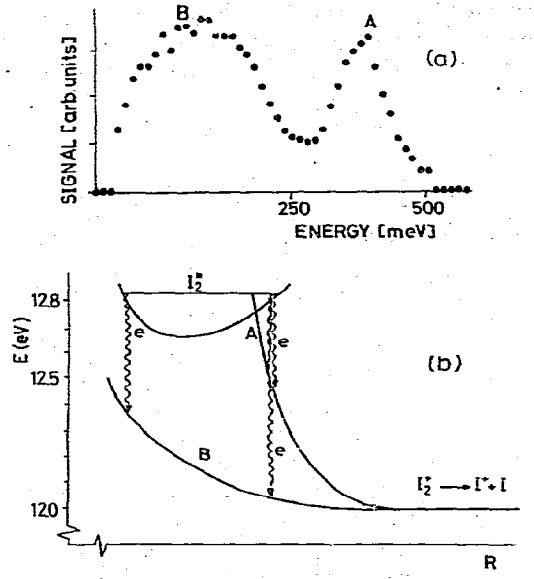

Fig. 3. (a) I^+ fragments as a function of their kinetic energy. The ions are formed in the two-photon (auto) ionization of I_2 by 193 nm radiation. (b) Potential curve model explaining I_2 autoionization data.

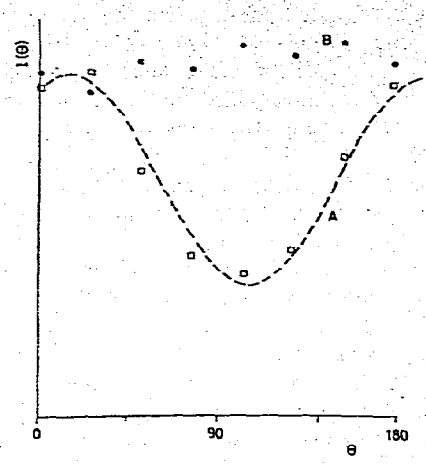

Fig. 4. Angular distributions of I^+ fragments with respect to the electric field vector upon 193 nm irradiation. A = fast ions, B = slow ions, as indicated in fig. 3a. The broken line is inserted for clarity.

220 mm distance. Large signals were obtained, disturbed by space charge, that will not be regarded here any further. In addition to those we also observed signals that were not affected by space charge. This could be checked by varying the beam density. It follows that those ions must have been formed after the space charge has been carried away by the ions that created it. This leads to the conclusion that the observed ions are due to autoionization from long lived Rydberg states. No negative ions are observed, which excludes the possibility of ion pair formation. On the other hand, a similar signal is observed of neutral fragments be it with poor signal to noise ratio. Fig. 3a shows the measured ion signal as a function of fragment kinetic energy. The dissociation limit of I_2^+ is 12.0 eV above the ground state of neutral I_2. The excess energies (twice the measured fragment energy) range from a few meV to about 0.85 eV. This is consistent with a two-photon process with an absorbed energy of 12.8 eV. Two peaks are observed. The high energy peak breaks off abruptly at the maximum available energy. We conclude that dissociative autoionization takes place through two repulsive I_2^+ curves, A and B, as indicated schematically in fig. 3b.

The fact that different I_2^+ curves are involved also follows from observation on the angular distribution of fragments with respect to the electric field vector. This was measured by rotating a polarizer, consisting of a stack of 10 quartz plates at Brewster's angle. The results are shown in fig. 4. The low energy ions are isotropically distributed, while the higher energy channel is distinctly anisotropic. The interpretation of such angular distribution of two-photon dissociation is straightforward only when axial recoil may be assumed [9]. This is clearly not the case here because the excited molecule may rotate many times before dissociation. We therefore confine ourselves to a simple qualitative model. We assume that the angular distribution of the heavy fragments is not affected by the step involving the departure of the electron. We then conclude that the molecule is excited to a number of bound excited states with different symmetries, of which some decay to A and the others to B.

4. Results and discussion — two lasers

In the experiments with two lasers neutral fragments as well as positive and negative ions were detec-

Table 1
Observed fragmentation processes

E_{laser} (eV)	Number of photons per wavelength			Fragments [a]	Observed [b]	E_{excess} (eV)	Angle scan	Delay scan	Remarks
	595	248	193						
12.48			2	$I^+ + I + e$	I, N	0 + 0.84	yes		auto-ionization
2.1	1			$I + I$	N	0.5			
4.2	2			$I' + I'$	N	0.7			
5		1		$I + I'$	N	2.5			
9.7	2	1		$I^+ + I^-(^1S)$	I	0.15		yes	
				$I' + I'$	N	5.8			
				$I + I'$	N	6.7			
12.1 + 5	1	2 + 1		$I^{+*} + I^* + e$	I, N	1.5–3		yes	(1)
14.2 + 5	2	2 + 1		$I^{+*} + I^* + e$	I	5		yes	(2)

[a] I indicates ground state $I(^2P_{3/2})$, I' is spin–orbit excited $I(^2P_{1/2})$, I^+ is ground state $I^+(^3P_2)$. States I^* and I^{+*} are unknown.
[b] I means ions are observed, N means neutrals are observed. Remarks: (1) The extra photon dissociates I_2^+. (2) The extra photon ionizes the I fragment.

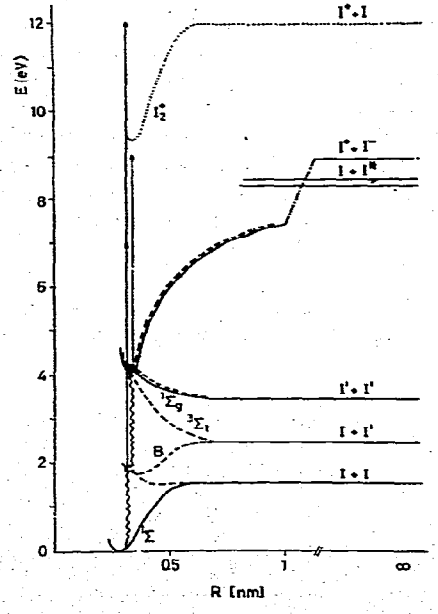

Fig. 5. Schematic potential curves of I_2 and I_2^+. Only those curves are indicated that are relevant to the present experiments. Solid curves have gerade symmetry, broken curves have ungerade symmetry. The dotted curve is I_2^+. Vertical lines indicate possible transitions in the experiment, with photon energies of 2.1 eV (initiating uplse) and 5 eV (probe pulse). I' indicates spin–orbit excited $I(^2P_{1/2})$.

ted, the latter ones with the multiplier at 69 mm. The initiating laser was operated at wavelengths between 600 and 580 nm. With one step the $B(^3\Pi_{0^+})$ state is formed. The probe laser wavelength was 248 nm. A variety of outgoing channels was observed, all summarized in table 1. The potential curves relevant to the present experiments are shown schematically in fig. 5. We will now discuss the major findings.

4.1. Intermediate states

Fig. 6 shows a time of flight spectrum of fragment ions with the initiating laser at 596 nm. Two peaks are distinguished that are due to fragments formed through different intermediate states. This can be seen from the variation of intensities with initiating laser wavelength. The low energy channel increases in intensity around 585 nm. It consists of two photon resonances, known as the Goodman band [7]. So this channel involves a two-photon intermediate state. On the other hand, the high energy channel has a one photon intermediate state. It has the same wavelength dependence as the one-photon absorption, as monitored by a reference cell. This is an important result since this technique permits us to distinguish between two simultaneously occurring processes. Additional information can be obtained with the help of the energy balance of eq. (1). Firstly the low energy peak is due to ion pair

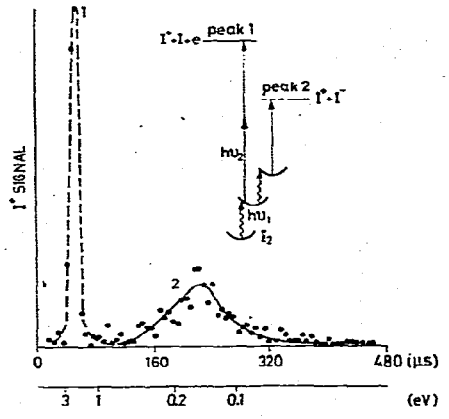

Fig. 6. Time of flight spectrum of ionic fragments upon multiphoton ionization of I_2 by 596 plus 248 nm. A schematic potential energy diagram is inserted. The broken line serves as a visual aid, the solid line is a computer simulation.

formation. The negative ions are observed equally well and at exactly the same flight times. This by the way proves the reliability of the energy measurement. The excess energy is 0.15 eV. This is consistent with a process involving a two-photon intermediate state and the absorption of one probe laser photon. The molecule subsequently dissociates into the energetically lowest possible ion pair channel with a dissociation limit of 8.93 eV [10]. The solid line in fig. 6 is a computer simulation assuming this process. Secondly, peak 1 — resulting from faster ions — is reproduced in more detail in fig. 7. The solid lines are computer simulations for excess energies of 1, 2 and 3 eV made with the assumption that no excess energy is carried off by a photoelectron. This assumption is clearly not valid, in particular for the lower energies. We conclude that ionization of the molecule is involved [reaction (III)]. This is consistent with a one-photon intermediate state and absorption of two probe laser photons to form bound I_2^+ (total absorbed energy 12.2 eV). The molecular ion is subsequently photodissociated by an additional photon. Due to the large number of possibilities for creating and dissociating I_2^+ no further attempt is made to assign the peaks in this process.

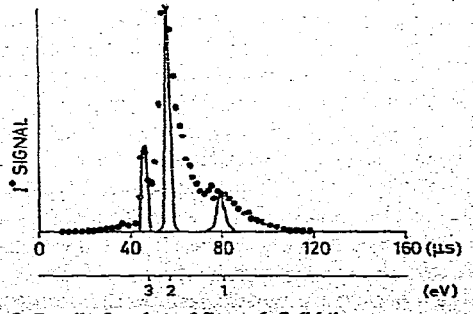

Fig. 7. Detail of peak 1 of figure 6. Solid lines are computer simulations for different energies, assuming no photoelectron to be produced in the process.

4.2. Lifetimes

By varying the delay between the two lasers the lifetimes of the intermediate states can be measured. We find for the two photon state a lifetime of 1.1 ± 0.1 μs, while the one photon intermediate state shows an apparent lifetime in the order of 3 μs. The B state, which is reached with one photon, has a known lifetime of the order of 1.5 μs [11]. However, we must consider the time evolution caused by the fact that the decay from the upper level (level 2) can repopulate the intermediate level (level 1) (see fig. 8). A rate equation is required in order to describe the time dependent population $N_1(t)$ of level 1 after excitation. We start with $N_1(0)$ particles in level 1 and $N_2(0)$ particles in level 2 (depending upon laser power) and write:

$$dN_1(t)/dt = -\Gamma_1 N_1(t) + \Gamma_2 N_2(0)\, e^{-\Gamma_2 t} ,$$

in which $1/\Gamma_1$ and $1/\Gamma_2$ are the lifetimes of level 1 and level 2 respectively. The solution can be written as

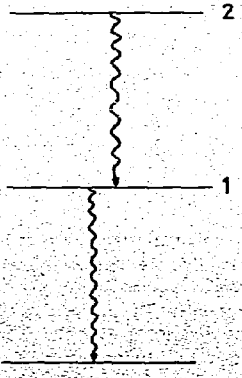

Fig. 8. Diagram indicating decay from two excited states.

follows: for $\Gamma_1 \neq \Gamma_2$:

$$N_1(t) = [N_1(0) - C]\, e^{-\Gamma_1 t} + C e^{-\Gamma_2 t},$$

with

$$C = \Gamma_2 N_2(0)/(\Gamma_1 - \Gamma_2),$$

for $\Gamma_1 = \Gamma_2$:

$$N_1(t) = N_1(0)\, e^{-\Gamma_1 t} + \Gamma_2 N_2(0)\, t\, e^{-\Gamma_2 t}.$$

From these equations it can be seen that for lifetimes and populations of the same order of magnitude the apparent lifetime of level 1 can be significantly enlarged. Of course the relative population of the two levels depends upon the laser parameters. Not only power and pulse duration are important, but also the bandwidth, which in the present case is 3 cm^{-1}.

4.3. Ion pair formation

The ion pair formation involved in peak 2 of fig. 6 results from predissociation of a long-lived excited state. This does not only follow from the fact that the signal is independent of ion density, like in the autoionization case. It also follows from the fact that negative ions are observed. The cross section for electron detachment of I^- at 248 nm is larger than 10^{-17} cm^2 [12]. This implies that any negative ion that is observed must have been formed after the gas laser pulse. Since we observe approximately the same amount of positive and negative ions this sets a lower limit of much longer than 20 ns to the lifetime of the dissociative state, which excludes the possibility of direct dissociation. The question to be answered is how can the highly excited Rydberg states couple with the ion pair forming state. As indicated in fig. 5 there are only two Rydberg states that can cross at large internuclear distance with the ion-pair state. Applying to them the scaling rules of Olson [13] we obtain the values of table 2. Here E_{max} is defined as the radial energy at which half of the particles would follow the adiabatic channel. It is clear that both crossings must be regarded as purely diabatic in the present case. This allows two possible explanations. First of all there is the possibility of a crossing at very short internuclear distances in the repulsive part of the potential. Secondly, one may assume that the Rydberg state is predissociated through another repulsive state, which crosses the ion pair state at much lower potential

Table 2
Crossings of diabatic I_2^* and $(I^+ + I^-)$ curves

Diabatic $(I^+ + I^-)$ state and energy at infinite internuclear distance (eV)	Diabatic I_2^* state $^2P_{3/2} + \ldots$	E [a] (eV)	R_c [b] (nm)	H_{12} [c] (meV)	E_{max} [d] (eV)
$I^+(^3P_2) + I^-(^1S)$ 8.93	$^4P_{5/2}$	8.31	2.4	5.5×10^{-4}	3.1×10^{-16}
	$^2P^o_{3/2}$	8.49	3.4	2.5×10^{-7}	5×10^{-29}
$I^+(^3P_{0,1}) + I^-(^1S)$ 9.73/9.81	$^4P_{5/2}$	8.31	1.0	21.6	25.3
	$^2P^o_{3/2}$	8.49	1.2	8.5	1.1
	$^4P_{1/2}$	9.09	2.3	6.9×10^{-3}	6.9×10^{-12}
$I^+(^1D) + I^-(^1S)$ 10.63	$^4P_{5/2}$	8.31	0.2	2.9×10^3	4.8×10^6
	$^2P^o_{5/2}$	8.49	0.7	234.5	7.7×10^4
	$^4P_{1/2}$	9.09	0.9	68.3	1.8×10^3
	$^4P_{3/2}$	9.20	1.0	47.3	594

[a] Energy of I_2^* at infinite internuclear distances.
[b] Crossing radius. [c] Interaction matrix element.
[d] Energy of nuclear motion, at which probabilities for diabatic and adiabatic passage of the crossing are equal. Values are calculated with scaling rules of Olson [13]. Only those states are indicated that are relevant in the case of excitation to 9.2 eV.

energy, and which therefore correlates with one of the lowest dissociation limits of the molecule. There are two arguments to support this latter assumption.

(a) One might expect high energy neutrals from dissociation along the diabatic path of the assumed crossing. They should have excess energies of 5.7 eV for dissociation into two spin–orbit excited fragments and 6.68 eV for one ground state and one spin–orbit excited fragment. Indeed, we observe those high energy peaks in the neutral spectrum, as shown in fig. 9. The peak designated G is due to dissociation by gas laser photons alone, via the $^3\Sigma_{1u}$ state. The peaks designated D and DD are due to the dye laser alone, in one step and two steps ($^1\Sigma_g$) respectively. The high energy peaks are observed only with both lasers on.

(b) A second argument can be derived from another photofragment experiment. Sander et al. [9] performed neutral photofragment spectroscopy on I_2 with two lasers at wavelengths in the visible. They measured the angular distribution of fragments dissociating from the $^1\Sigma_g$ state. The result did not agree with the predicted $\cos^2\theta$ distribution, which can be explained by the presence of a predissociating state, in agreement with our present model.

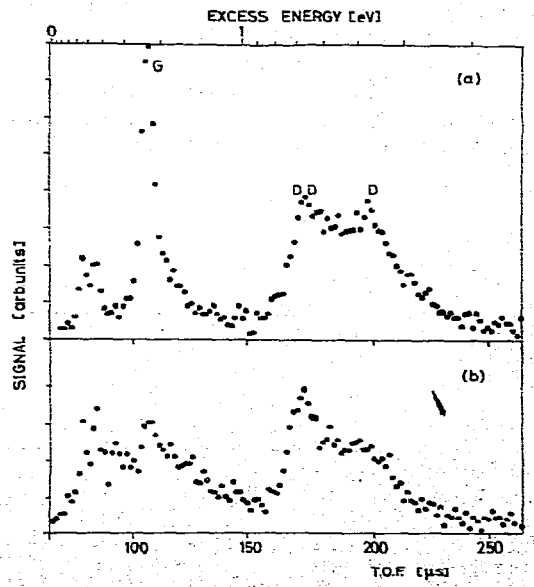

Fig. 9. (a) Time of flight spectrum of neutral fragments upon multiphoton ionization of I_2 by 596 plus 248 nm. Indication of peaks is explained in the text. (b) Same as (a), but with 248 nm light polarized with electric field vector parallel to direction of detection. Also the intensity of the 596 nm light is higher, leading to a stronger depopulation of the intermediate level that leads to peak D. Peak G is due to a perpendicular transition (the only allowed ungerade state is $^3\Pi_1$). By the choice of polarization it is "filtered out", revealing another signal. This is the neutral counterpart of the 1.5–3 eV ion signal reported in the text.

All these arguments imply that the lowest ion pair states must have a potential energy lower than previously has been assumed. At least one gerade state can be reached with two times 2.1 eV and there are indications for crossings with repulsive states at larger R, rather than at very small R.

5. Conclusions

The experiments reported here show that multiphoton ionization translational spectroscopy (MITS) can serve to obtain information about (i) the dynamics of multiphoton ionization and (ii) highly excited repulsive states. In the one-laser experiment dissociative autoionization is observed. The process proceeds simultaneously along two channels that are distinguished by fragment kinetic energy and angular distribution. In the two laser experiments there are two major conclusions. In the first place two competing processes are distinguished that proceed through different intermediate states. By varying the time delay between initiating and probe laser we followed the time evolution of those intermediate states and measured their lifetimes. This may offer possibilities for future experiments to gain information on the two photon excitation process itself. A question to be answered might be: what laser parameters influence the probability for either one or two photon excitation? The second conclusion to be drawn is based on our ability to observe both ionic and neutral fragments. This leads to a reinterpretation of potential curves using a model with curve crossings of the lowest ion pair states with repulsive neutral curves.

We believe that these are the first examples of the application of a new technique. It is still open to refinement – e.g. by improved resolution or by measuring photoelectrons in coincidence – and it should be helpful in providing information about multiphoton ionization processes and about the highly excited repulsive states involved with them.

Acknowledgement

We are indebted to Professors M.J. van der Wiel, Y.T. Lee and R.B. Bernstein for stimulating discussions. This work is part of the research program of the Stichting voor Fundamenteel Onderzoek der Materie (Foundation for Fundamental Research on Matter) and was made possible by financial support from the Nederlandse Organisatie voor Zuiver-Wetenschappelijk Onderzoek (Netherlands Organization for the Advancement of Pure Research).

References

[1] D.H. Parker, J.O. Berg and M.A. El-Sayed, in: Advances in laser chemistry, ed. A.H. Zewail (Springer, Berlin, 1978).
[2] C.B. Collins, B.W. Johnson, D. Popescu, G. Musa, M.L. Pascu and I. Popescu, Phys. Rev. A8 (1973) 2197.
[3] A. Herrmann, S. Leutwyler, E. Schumacher and L. Wöste, Chem. Phys. Letters 52 (1977) 418.
[4] M. Klewer, M.J.M. Beerlage, J. Los and M.J. van der Wiel, J. Phys. B10 (1977) 2809.
[5] R.S. Mulliken, J. Chem. Phys. 55 (1971) 288;
K. Wieland, J.B. Tellinghuisen and A. Nobs, J. Mol. Spectry. 41 (1972) 60;
J.A. Coxon, Molecular spectroscopy, Vol. 1 (The Chemical Society, London, 1973) pp. 177 ff;
J. Tellinghuisen, Chem. Phys. Letters 49 (1977) 485;
J.C. Lehmann, Rec. Prog. Phys. 41 (1978) 1609.
[6] (a) G. Petty, C. Tai and F.W. Dalby, Phys. Rev. Letters 34 (1975) 1207;
(b) M.D. Danyluk and G.W. King, Chem. Phys. 22 (1975) 59;
(c) C. Tai and F.W. Dalby, Can. J. Phys. 56 (1978) 183;
(d) L. Zandee and R.B. Bernstein, J. Chem. Phys. 71 (1979) 1359;
(e) M. Kawasaki, K. Tsukiyama, M. Kuwana, K. Obi and I. Tanaka, Chem. Phys. Letters 67 (1979) 365;
(f) A.D. Williamson and R.N. Compton, to be published.
(g) K.K. Lehmann, J. Smolarek and L. Goodman, J. Chem. Phys. 69 (1978) 1569.
[7] D.E. Nitz, P.B. Hogan, L.D. Schearer and S.J. Smith, J. Phys. B12 (1979) L103.
[8] M.S. de Vries, N.J.A. van Veen, M. Hutchinson and A.E. de Vries, Chem. Phys. 51 (1980) 159.
[9] R.K. Sander, Ph. D. Thesis, University of California (1974).
[10] J.A. Meyer and J.A.R. Samson, J. Chem. Phys. 52 (1969) 716.
[11] J. Vigué, Ph. D Thesis, University of Paris (1978).
[12] A. Mandl and H.A. Hyman, Phys. Rev. Letters 31 (1973) 417.
[13] R.E. Olson, F.T. Smith and E. Bauer, Appl. Opt. 10 (1971) 1248.
[14] M.S. de Vries, Ph. D. Thesis University of Amsterdam, The Netherlands (1980).